Chemical Geology 324-325 (2012) 46–58

Contents lists available at SciVerse ScienceDirect

Chemical Geology

journal homepage: www.elsevier.com/locate/chemgeo

Research paper

Analysis of marine environmental conditions based on molybdenum–uranium covariation—Applications to Mesozoic paleoceanography

N. Tribovillard [a,*], T.J. Algeo [b], F. Baudin [c], A. Riboulleau [a]

[a] Université Lille 1, Laboratoire Géosystèmes, FRE CNRS 3298, bâtiment SN5, 59655 Villeneuve d'Ascq cedex, France
[b] Department of Geology, University of Cincinnati, Cincinnati, Ohio 45221-0013, USA
[c] UPMC—Univ. Paris 06 et CNRS UMR 7193 ISTeP, Case courrier 117, 4 place Jussieu, 75252 Paris Cedex 05, France

ARTICLE INFO

Article history:
Accepted 13 September 2011
Available online 17 September 2011

Keywords:
Sedimentary geochemistry
Redox conditions
Anoxia
Oceanic anoxic event
Jurassic
Cretaceous

ABSTRACT

Patterns of uranium–molybdenum covariation in marine sediments have the potential to provide insights regarding depositional conditions and processes in paleoceanographic systems. Specifically, such patterns can be used to assess bottom water redox conditions, the operation of metal-oxyhydroxide particulate shuttles in the water column, and the degree of water mass restriction. The utility of this paleoenvironmental proxy is due to the differential geochemical behavior of U and Mo: (1) uptake of authigenic U by marine sediments begins at the Fe(II)–Fe(III) redox boundary (i.e., suboxic conditions), whereas authigenic Mo enrichment requires the presence of H_2S (i.e., euxinic conditions), and (2) transfer of aqueous Mo to the sediment may be enhanced through particulate shuttles, whereas aqueous U is unaffected by this process. In the present study, we examine U–Mo covariation in organic-rich sediments deposited mostly in the western Tethyan region during oceanic anoxic events (OAEs) of Early Jurassic to Late Cretaceous age. Our analysis generally confirms existing interpretations of redox conditions in these formations but provides significant new insights regarding water mass restriction and the operation of particulate shuttles in depositional systems. These insights will help to address contentious issues pertaining to the character and origin of Mesozoic OAEs, such as the degree to which regional paleoceanographic factors controlled the development of the OAEs.

1. Introduction

Trace metals are commonly used for paleoenvironmental reconstruction, especially redox-sensitive and/or sulfide-forming elements that may become strongly enriched under low-oxygen and/or sulfidic water mass conditions. Among such elements, uranium (U) and molybdenum (Mo) have been extensively studied (Emerson and Huested, 1991; Klinkhammer and Palmer, 1991; Wignall, 1994; Crusius et al., 1996; Helz et al., 1996; Dean et al., 1999; Morford and Emerson, 1999; Erickson and Helz, 2000; Zheng et al., 2000, 2002a, 2002b; Chaillou et al., 2002; Bostick et al., 2003; Lyons et al., 2003; Algeo and Maynard, 2004; Tribovillard et al., 2004; Vorlicek et al., 2004; McManus et al., 2005; Morford et al., 2005; Brumsack, 2006; McManus et al., 2006; Tribovillard et al., 2006, 2008a, 2008b; Lyons et al., 2009; Morford et al., 2009; Piper and Calvert, 2009; Poulson Brucker et al., 2009). These two trace metals are especially useful for paleoenvironmental reconstructions owing to their geochemical properties and behavior: (1) both are present in low concentrations in the upper continental crust (U ~2.7 ppm, Mo ~3.7 ppm; McLennan, 2001) and transferred to the ocean mainly by fluvial input; (2) both are present in low concentrations in marine plankton; (3) both have long residence times in seawater (U ~450 kyr, Mo ~780 kyr) and, hence, nearly uniform aqueous concentrations throughout the global ocean; and (4) both exhibit conservative behavior under oxic conditions but enhanced uptake by the sediment where the water mass is anoxic. As a consequence of these characteristics, enrichments of U and Mo in sediments or sedimentary rocks may generally be imputed to authigenic uptake of these elements from seawater.

The mechanisms of authigenic enrichment are somewhat different for U and Mo (for a detailed discussion, see Algeo and Maynard (2004), Tribovillard et al. (2006), Algeo and Tribovillard (2009), and references therein). The main mechanism by which aqueous U is removed from seawater is uptake across the sediment–water interface in reducing facies. Under conditions close to those required for conversion of Fe^{3+} to Fe^{2+}, soluble U(VI) is reduced, possibly through microbial mediation, to insoluble U(IV). In this state, U removal to the sediment may be accelerated by the formation of organometallic ligands and by enhancing the influence of organic substrates on U uptake. The accumulation is (at least partly) mediated by bacterial sulfate reduction reactions, because without bacterial activity, the reduction

* Corresponding author.
E-mail address: Nicolas.Tribovillard@univ-lille1.fr (N. Tribovillard).

0009-2541/$ – see front matter © 2011 Elsevier B.V. All rights reserved.
doi:10.1016/j.chemgeo.2011.09.009

process seems to be very slow (McManus et al., 2005, and references therein). Mo is also likely to be taken up across the sediment–water interface under reducing conditions (Zheng et al., 2000). However, removal of Mo to the sediment requires formation of particle-reactive thiomolybdates ($MoO_xS^{2-}_{4-x}$, where x = 0 to 3), which are then scavenged by sulfidized (S-rich) organic material or Fe–S phases (Tribovillard et al., 2004). Thiomolybdate formation occurs only in the presence of free hydrogen sulfide (H_2S) (Helz et al., 1996, 2011) and, thus, at a lower redox potential than that for sedimentary uptake of U, creating the potential for enhanced uptake of U relative to Mo where suboxic conditions prevail (Algeo and Tribovillard, 2009). A second difference between the behavior of U and Mo is that the latter element is vigorously scavenged by metal oxyhydroxides (especially MnOOH but including FeOOH), probably in relation to a speciation change from the dissolved MoO_4^{2-} to the particle reactive MoO_3 (Tossell, 2005). Particulate Mn-oxides adsorb molybdate oxyanions during transit through the water column, playing the role of a shuttle (Algeo and Tribovillard, 2009; Dellwig et al., 2010). Usually, upon reaching the sediment/water interface, these particles are reductively dissolved, releasing molybdate ions that then either diffuse back into the water column or are scavenged by other phases within the sediment.

In a recent paper, Algeo and Tribovillard (2009) used these differences in the geochemical behavior of U and Mo to demonstrate how patterns of authigenic U–Mo co-variation may be related to specific redox conditions and processes in marine depositional systems. These authors, using enrichment factors (EFs; see definition in Section 2.2), identified three patterns of U–Mo covariation, each associated with a different modern marine setting. First, sediments of the eastern tropical Pacific exhibit a pattern of greater relative U_{auth} enrichment (Mo:U ratios of ~0.1 to 0.3 × SW) at low EFs, indicative of suboxic conditions, and progressively greater relative Mo_{auth} enrichment (Mo:U ratios >1 × SW) at high EFs, indicative of a shift toward more intense and/or sustained anoxia in the water column (Fig. 1A). This trend is characteristic of "unrestricted marine" settings (Fig. 1B). Second, sediments of the Cariaco Basin exhibit strong enrichment of Mo relative to U at all EFs, reflecting the operation of a metal-oxyhydroxide particulate shuttle that enhances the export of aqueous Mo to the sediment (with little effect on aqueous U; Fig. 1A). Mo:U ratios are generally much greater (3 to 10 × SW) than the seawater ratio, defining a "particulate shuttle" trend that is distinct from the unrestricted marine trend (Fig. 1B). Finally, Algeo and Tribovillard (2009) identified a third pattern, characterized by decreasing Mo:U ratios with increasing EFs. This pattern is characteristic of sediments of the modern Black Sea and is inferred to represent the influence of changes in water mass chemistry with water depth (n.b., the deepwater mass of the Black Sea contains ~70% of the seawater concentration of U but only ~3% of the Mo concentration; Algeo and Maynard, 2008). This pattern, development that requires an extended interval of deepwater isolation to allow chemical evolution of the water mass, was tentatively identified in some Devonian black shales by Algeo and Tribovillard (2009).

In the present paper, we extend the ideas developed in Algeo and Tribovillard (2009) to an analysis of depositional conditions and processes in organic-rich units of Mesozoic age (Fig. 2). The Mesozoic experienced multiple episodes of oceanic anoxia commonly extending across broad portions of the Tethys Ocean and sometimes developed concurrently in the Panthalassic/Paleo-Pacific Ocean and in epicratonic seas. These episodes, termed Oceanic Anoxic Events (OAEs), were more or less protracted, ranging from a few thousand years to several million years in duration. They were commonly limited to oceanic deepwaters but sometimes impinged on the platform domain, depending on the paleogeographical configuration and other paleoceanographic factors (see the recent review by Jenkyns (2010)). The OAEs and other episodes of extensive organic matter storage studied here are the Toarcian OAE-T (Early Jurassic), the Kimmeridgian and early Tithonian (Late Jurassic), the Hauterivian (Early Cretaceous), and the Cenomanian–Turonian OAE-2 and Coniacian–Santonian OAE-3 (Middle to Late Cretaceous; Fig. 2). We chose to examine geological formations that have already been well studied because we intend to (1) test the robustness of U–EF vs. Mo–EF covariation as a proxy for paleoredox conditions and processes that were previously interpreted using independent parameters, and (2) determine whether U–EF vs. Mo–EF covariation provides new insights regarding the paleoceanography of these organic-rich depositional systems.

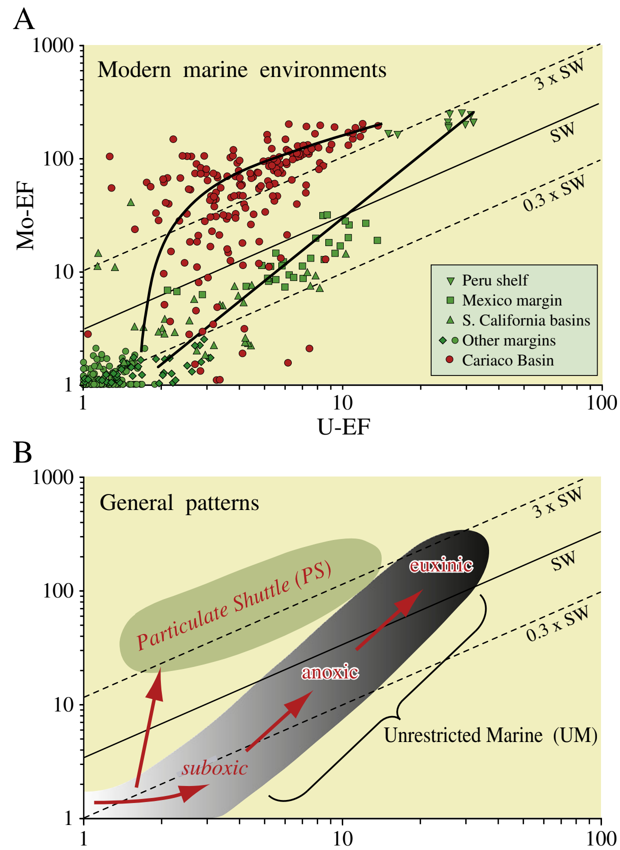

Fig. 1. (A) U–EF vs. Mo–EF for modern marine environments. Samples are from unrestricted marine facies of the eastern tropical Pacific (green symbols) and the restricted Cariaco Basin (modified from Algeo and Tribovillard (2009)). The heavy solid lines highlight the pattern of U–Mo covariation in each environment. The eastern tropical Pacific is subject to a wide range of bottom water redox conditions, including fully oxic along the Chilean margin, suboxic to episodically anoxic along the California and Mexican margins, and perennially anoxic within depressions of the Peru margin. Redox variation among these settings shows a strong relationship to the degree of authigenic U–Mo enrichment. Data from McManus et al. (2006). EF = enrichment factor (see Eq. (1) in the text). The diagonal lines represent multiples (0.3, 1, and 3) of the Mo:U ratio of present-day seawater: molar ratios of ~7.5 for the Pacific and ~7.9 for the Atlantic have been converted to an average weight ratio of 3.1 for the purpose of comparison with sediment Mo:U weight ratios. (B) General patterns of U–EF vs. Mo–EF covariation in modern marine environments. The gray field represents the "unrestricted marine" (UM) trend, characteristic of the eastern tropical Pacific, whereas the green field represents the "particulate shuttle" (PS) trend, characteristic of depositional systems such as the Cariaco Basin in which intense redox cycling of metal (especially Mn—) oxyhydroxides occurs within the water column.

2. Material and methods

2.1. Study units

Here we study the respective EF of U and Mo of well-known geological formations ranging in age from the Early Jurassic to the Late Cretaceous and mostly from the western Tethyan region. Only their main features are summarized here, but we provide references where more

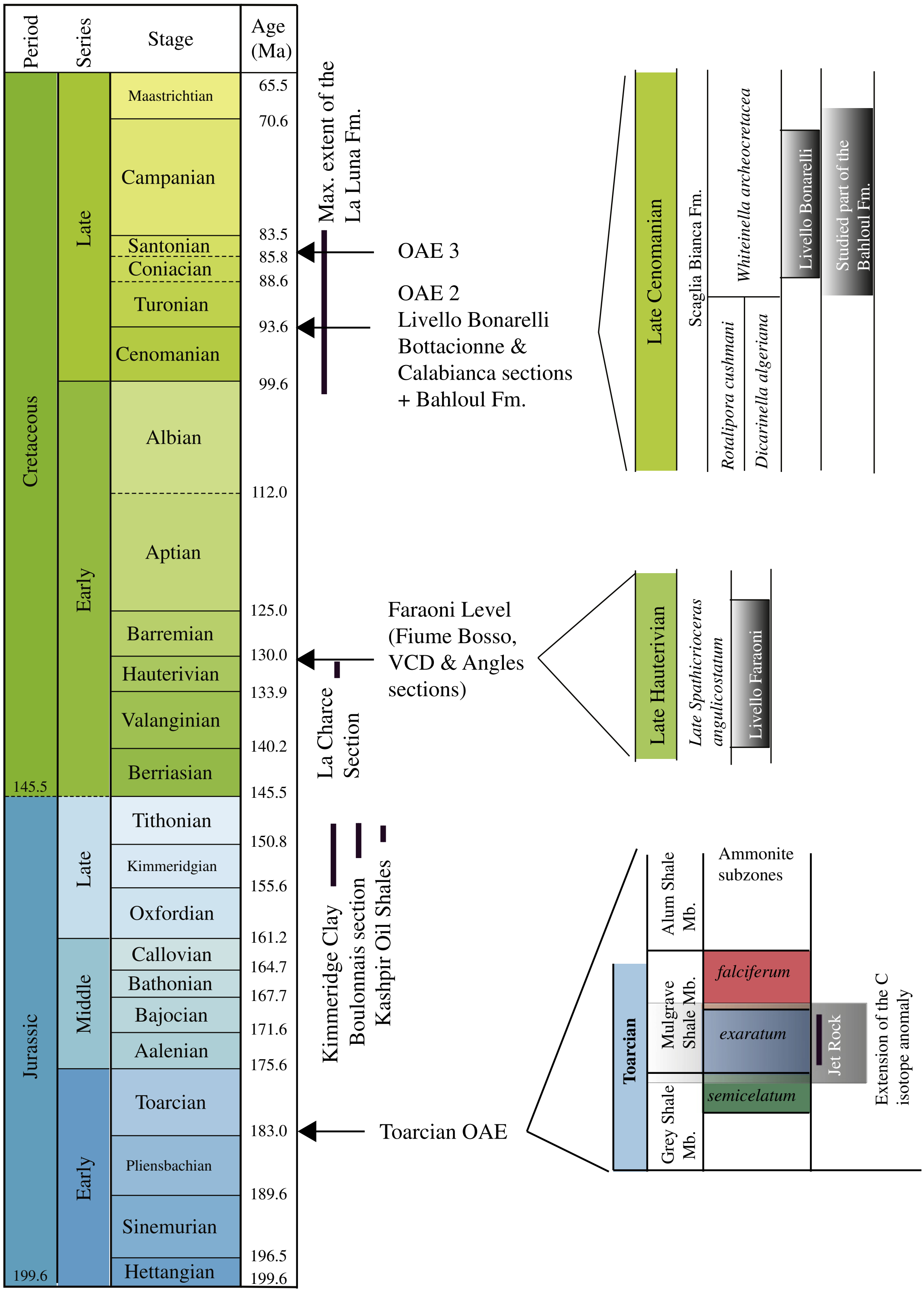

Fig. 2. Stratigraphic distribution of the oceanic anoxic events (OAE) and organic matter-rich formations studied in the present paper. Time scale after the International Stratigraphic Chart 2009.

complete descriptions are available. These ancient sediments (carbonates, marls and shales) were deposited under suboxic to anoxic or even strongly euxinic conditions, based on independent paleoredox criteria described in each supporting paper. All contain detectable to abundant amounts of organic matter of predominantly marine origin.

2.1.1. Early Jurassic

The ~183-Ma Toarcian OAE (Fig. 2) is documented by negative C-isotope excursions in sections with a near-global distribution (Cohen et al., 2004) as well as by excursions in other proxies indicative of changes in global seawater composition (Jenkyns et al., 2002; Wignall et al., 2005; Pearce et al., 2008; Suan et al., 2008, 2010). These organic-rich shales were deposited in semi-restricted basins surrounded by shallow shelf seas extending across the West European platform to the north of the Tethys Ocean (Fig. 3A). McArthur et al. (2008) showed that the degree of water restriction varied regionally, being strongest in areas that were deeper and more distant from the Tethys Ocean (such as the Cleveland Basin; Yorkshire, UK) and less restricted toward the south and east across the West European platform. The upper Pliensbachian–lower Toarcian shales of the Cleveland Basin encompass a protracted episode of extreme water mass seclusion, with a total duration between 200 and 900 kyrs (McArthur et al., 2008; Suan et al., 2008). In the present study, we utilize analytical data from McArthur et al. (2008; Fig. 2).

2.1.2. Late Jurassic

During the Late Jurassic, major organic matter accumulations developed in middle and high latitudes of the northern hemisphere,

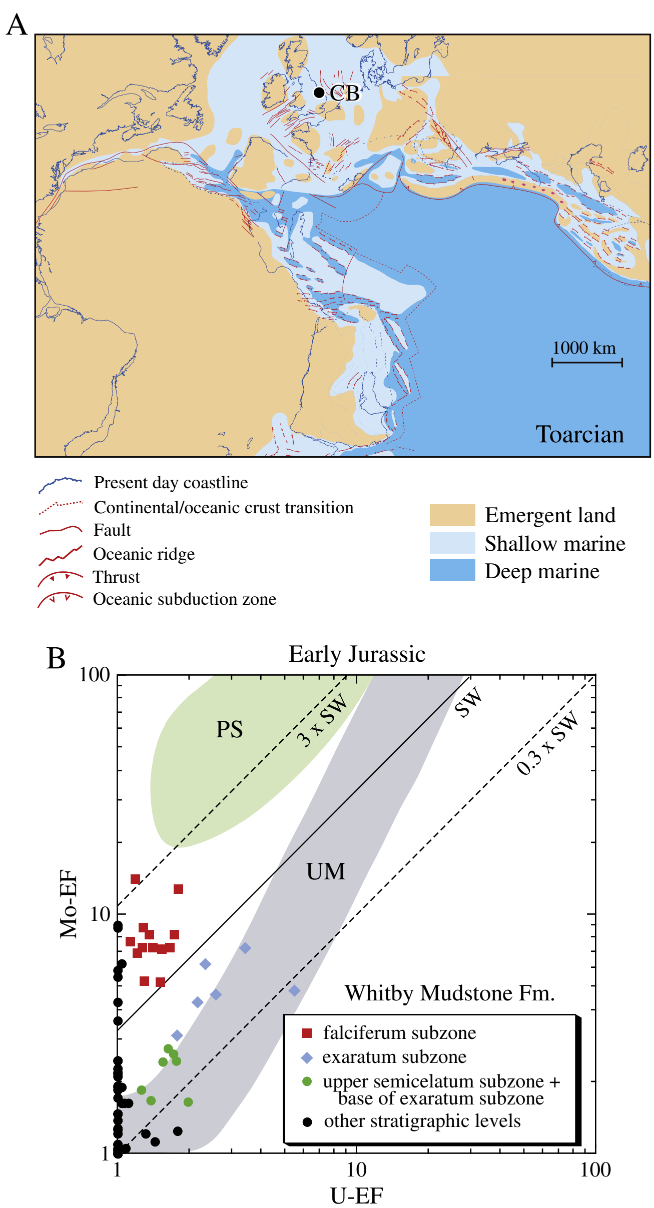

Fig. 3. (A) Paleogeographic reconstruction of the western Tethyan region during the Toarcian (Early Jurassic) showing the location of the Cleveland Basin (CB; Yorkshire, United Kingdom). Redrawn from Barrier and Vrielynck (2008). (B) U–EF vs. Mo–EF for late Pliensbachian–early Toarcian samples of the Whitby Mudstone Formation. Data from McArthur et al. (2008). Abbreviations as in Fig. 1.

associated with the Kimmeridge Clay Formation of the North European Platform, with the Bazhenov Formation in the Western Siberian basin, and with marine formations in the circum-Arctic basins of North Alaska, the Sverdrup Basin, and the Barents Sea (Riboulleau et al., 2003). Located between these large domains, the Russian Platform was covered by a shallow epicontinental sea that was also characterized by extensive organic matter deposition.

The Late Jurassic Kimmeridge Clay Formation (KCF) was deposited across a large part of northern Europe between ~155 and 148 Ma (Fig. 2; see recent synthetic papers by Piper and Calvert (2009) and Pearce et al. (2010), and references therein). The KCF was deposited in a series of shallow basins included in the epicontinental Laurasian seaway that connected the Boreal and Tethyan oceans (Fig. 4A). In this paper, we consider the KCF of the Cleveland Basin of Yorkshire (United Kingdom). These deposits accumulated in the distal part of the epicontinental sea extending from the Barents Sea to the English Channel. The cored sections of the Cleveland Basin show alternations of shales, marls and clayey limestones deposited under variably O_2-depleted (i.e., suboxic to euxinic) conditions. However, Pearce et al. (2010) concluded that no indication of water mass stagnation or restriction could be observed.

Cycles of organic matter enrichment on several scales (from the lamina to the Milankovitch frequency band) are a prominent feature of the KCF (Tribovillard et al., 2005; Tyson, 2005). The present paper focuses on three well-studied meter-scale cycles (Ramanampisoa et al., 1992; Tribovillard et al., 1994; Lallier-Vergès et al., 1997; Tribovillard et al., 2005). Cycle 1 yields TOC values of 2–10% (consisting of a mixture of terrestrial and marine organic matter) and corresponds to suboxic conditions of deposition. Cycle 2 yields TOC values of 4–31% (consisting predominantly of marine organic matter) and corresponds to euxinic conditions of deposition. It contains several layers that are rich in sulfurized organic matter. Cycle 3 yields TOC values of 2–20% and is intermediate in terms of organic matter character and depositional redox conditions between those of cycles 1 and 2.

Late Jurassic sediments of the Boulonnais area of northern France include the Argiles de Wimereux and Bancs Jumeaux formations (Fig. 4A). The Kimmeridgian Argiles de Châtillon Formation consists of dark marls, mudstones, and shales containing abundant organic matter mainly of marine and secondarily of terrigenous origin with strong sulfurization of the former in samples containing TOC >6–7%. These sediments were deposited in a hemi-pelagic setting that was variably oxic to anoxic. The Tithonian-age Argiles de Wimereux and Bancs Jumeaux formations consist of dark marls, mudstones, and siltstones containing low to moderate amounts of organic matter predominantly of terrigenous and secondarily of marine origin. These sediments were deposited on a mixed carbonate–siliciclastic ramp under redox conditions ranging from normally oxygenated to suboxic. Previous studies have inferred largely oxic conditions for the Argiles de Wimereux Formation and suboxic condtions for the Bancs Jumeaux Formation (Proust et al., 1995; Deconinck et al., 1996; Tribovillard et al., 2001; Wignall and Newton, 2001; Tribovillard et al., 2002, 2005, 2008a).

A major episode of organic matter accumulation occurred on the Russian Platform (from the Pechora Basin in the north to the Peri-Caspian Depression in the south, and into the Moscow Basin; Fig. 4A) during the latest Jurassic (Middle Volgian or latest Early Tithonian; Fig. 2). This short event resulted in organic-rich deposits that are relatively thin (8–10 m) but of nearly uniform thickness and facies character across the platform. In the middle Volga Basin, the organic-rich deposits from the *Dorsoplanites panderi* ammonite zone are known as the Kashpir Oil Shales (Riboulleau et al., 2003, and references therein). These units made up with meter-scale alternations of organic-rich black shale and organic--poor marls and calcareous claystones accumulated under bottom water redox conditions that were frequently oxygenated. However, beds that are particularly rich in sulfurized organic matter (TOC to 45%) represent the transient development of euxinic conditions (Riboulleau et al., 2003).

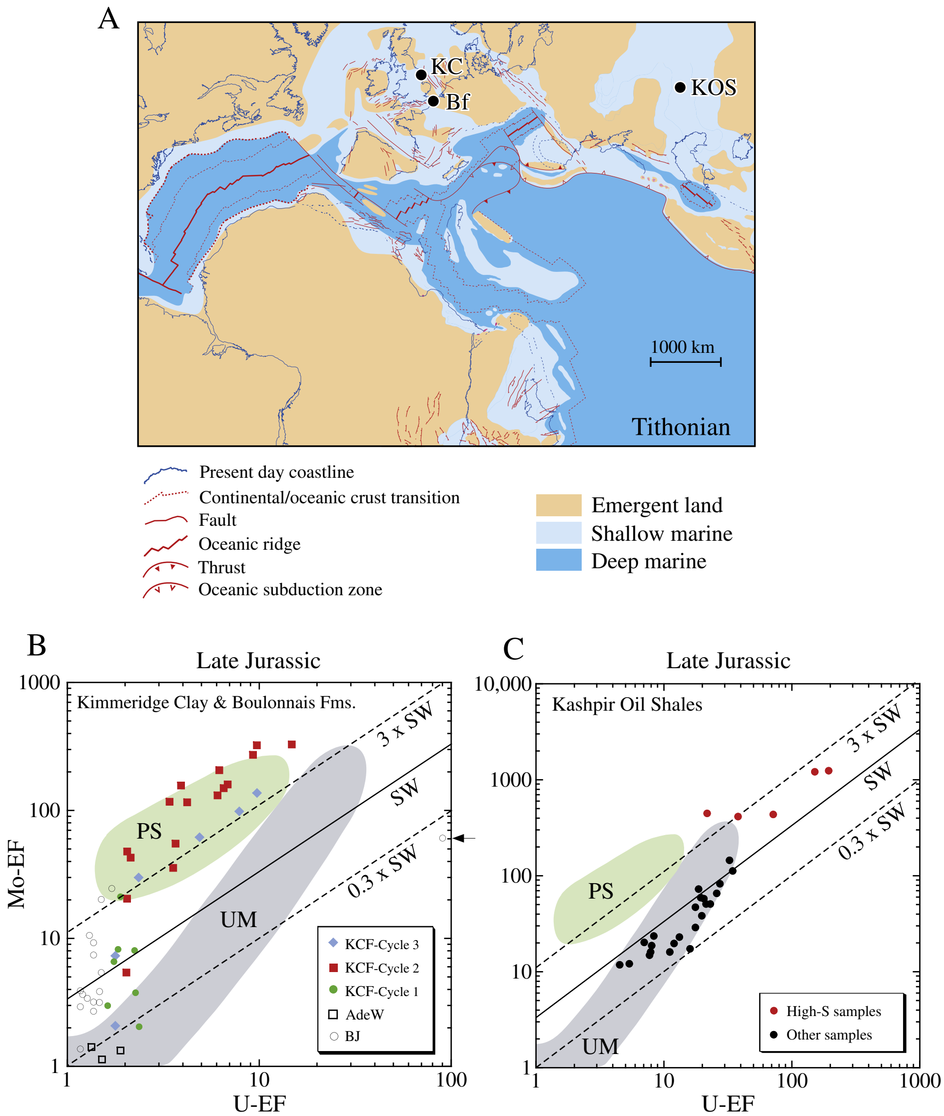

Fig. 4. (A) Paleogeographic reconstruction of the western Tethyan region during the Tithonian (Late Jurassic) showing the locations of the Kimmeridge Clay (KC; Yorkshire, United Kingdom), Boulonnais formations (Bf; northern France), and Kashpir Oil Shales (KOS; Kazakhstan). Redrawn from Barrier and Vrielynck (2008). (B) U–EF vs. Mo–EF for the Kimmeridge Clay Formation (Cycles 1 to 3) and the Argiles de Wimereux (AdeW) and Bancs Jumeaux (BJ) formations of the Boulonnais region. Data from Tribovillard et al. (2005). (C) U–EF vs. Mo–EF for the Late Jurassic (Volgian) Kashpir Oil Shales of the Russian Platform. Data from Riboulleau et al. (2003). Abbreviations as in Fig. 1.

2.1.3. Early Cretaceous

A short-lived episode of oxygen-deficient marine conditions, termed the Livello Faraoni, developed during the latest Hauterivian (late *Spathicrioceras angulicostatum* ammonite zone; Fig. 2). This organic-rich horizon was identified in the Umbria–Marche Basin of Central Italy and at various sites in the Western Tethys Ocean: the Trento Plateau of Italy, the Vocontian Trough of SE France, and the Swiss Prealpes (Cecca et al., 1994; Baudin et al., 1999; Bodin et al., 2007). The Livello Faraoni may be linked to a coeval drowning event that affected northern Tethyan carbonate platforms (Bodin et al., 2007).

In this paper, we examine three (hemi-) pelagic sections forming a N–S transect through the western Tethys (Fig. 5A), where the Hauterivian–Barremian transition is recorded mainly by micritic limestones and marls (Bodin et al., 2007). In the Fiume-Bosso Section, located between Urbino and Gubbio (central Italy), the Livello Faraoni appears as three laminated black shale layers within pelagic limestones and cherts of the Maiolica Formation. During the latest Hauterivian, this section was situated in the southern part of the Tethys, within the deep Umbria–Marche Basin. The Veveyse de Châtel-Saint-Denis (VCD) Section is located along the Veveyse River close to Fribourg (Switzerland), where the Livello Faraoni consists of organic-rich shales and marly limestones. The Angles Section is located near Barrême (southeastern France), where the Livello Faraoni is expressed as laminated shales within a limestone–marl succession. During the latest Hauterivian, these sections were located on the northern Tethyan margin, either within the Vocontian Trough (Angles) or in the adjacent Ultra-Helvetic realm, a deep northeastern elongation of the Vocontian Trough (VCD). We also examined the La Charce section (Vocontian Basin, southeastern France), which represents a pelagic setting with oxic to suboxic bottom waters (Fig. 5A). This section records typical pelagic alternations of burrowed limestone beds and marls (Baudin et al., 1999; Van de Schootbrugge et al., 2000, 2003). The La Charce section covers the Late Hauterivian but does not expose the time-equivalent of the Faraoni Level.

2.1.4. Middle to Late Cretaceous

The famous OAE-2, bracketing the ~93-Ma Cenomanian–Turonian boundary (Fig. 2) was a short (220–800 kyr) anoxic event characterized

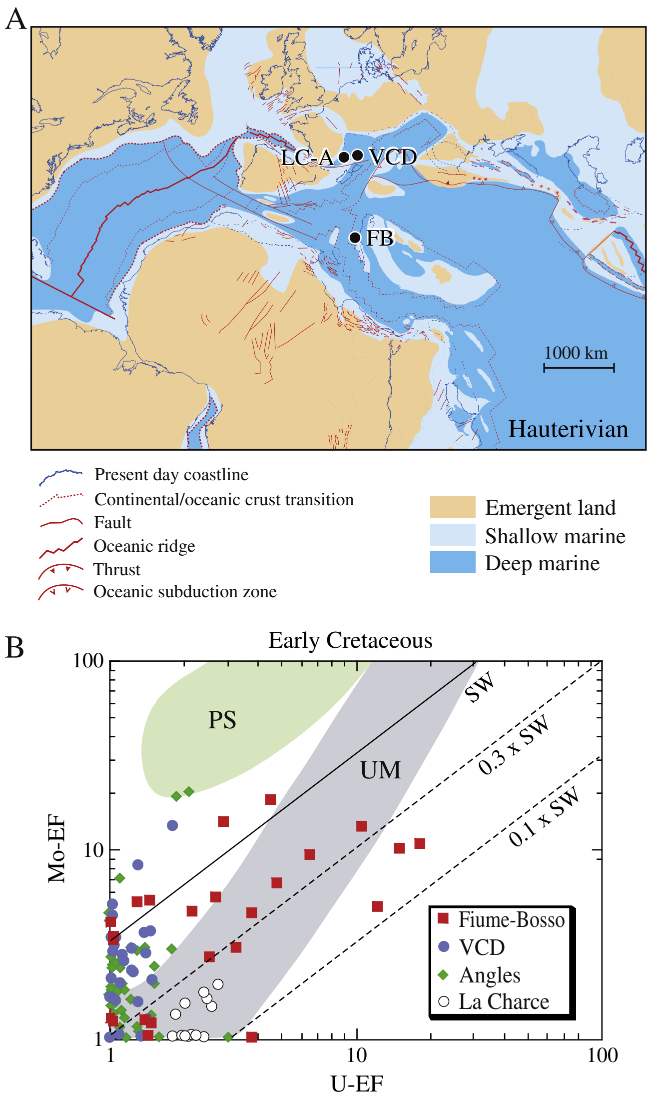

Fig. 5. (A) Paleogeographic reconstruction of the western Tethyan region during the Hauterivian (Early Cretaceous) showing the locations of the La Charce and Angles (LC–A) sections of the Vocontian Trough (France), the Veveyse-Châtel-Saint-Denis (VCD) section (Switzerland), and the Fiume-Bosso (FB) section (Italy). Redrawn from Barrier and Vrielynck (2008). (B) U–EF vs. Mo–EF for Hauterivian samples from the four sections listed in A. Data from Bodin et al. (2007). Abbreviations as in Fig. 1.

by enhanced marine productivity in the Tethyan regions (e.g., Brumsack, 2006; Scopelliti et al., 2006; Turgeon and Brumsack, 2006; Jenkyns, 2010). Enhanced productivity resulted in dysoxic to anoxic bottom waters over wide areas, intensifying to euxinia at the peak of the event, when anoxia was widespread in the deeper parts of the Tethys as well as in shallow shelf environments. One of the most studied expressions of the OAE-2 is a horizon called the Livello Bonarelli, which appears in the Bottaccione Section of the Umbria–Marche Basin (Gubbio area, central Italy; Fig. 6A). The Livello Bonarelli consists of a 1 m-thick horizon of organic-rich shales interspersed with radiolarian-rich beds, in sharp contrast to under- and overlying siliceous limestone beds of the Scaglia Bianca Formation (Scopelliti et al., 2006; Turgeon and Brumsack, 2006). The Calabianca Section of northwestern Sicily contains the age-equivalent horizon (Scopelliti et al., 2006). Both sections were deposited at bathyal depths within the Tethys Ocean: ~1500–2500 m for Bottaccione and somewhat shallower for Calabianca (Scopelliti et al., 2004). Both locations experienced high surface water productivity and anoxic benthic conditions, but productivity was stronger in the Sicilian area, which was under the influence of an upwelling system along the south Tethyan margin. Consequently, benthic redox conditions were more reducing at Calabianca, where euxinia existed in the water column, than at Bottaccione (Scopelliti et al., 2006).

The Bahloul Formation of Tunisia represents OAE-2 sedimentation on a shallow platform (Fig. 6A; Caron et al., 1999; Soua and Tribovillard, 2007). This formation that can be traced from the margin of the Saharan platform (southern Tunisia) to the deep Tethyan Basin to the north, shows regular alternations of black laminated limestone beds and bioturbated grey marls. The black laminated facies was deposited under suboxic to anoxic conditions, whereas the grey marls were deposited under more frequently oxygenated conditions (Caron et al., 1999).

The famous oil-source rock La Luna Formation was deposited during a major Late Cretaceous transgression of the northern margin of South America (Fig. 6A; Marcellari and De Vries, 1987; Tribovillard et al., 1991; Erlich et al., 1999a, 1999b; Alberdi and Tocco, 1999; Erlich et al., 2000; Lo Mónaco et al., 2002; Rey et al., 2004). The formation ranges in

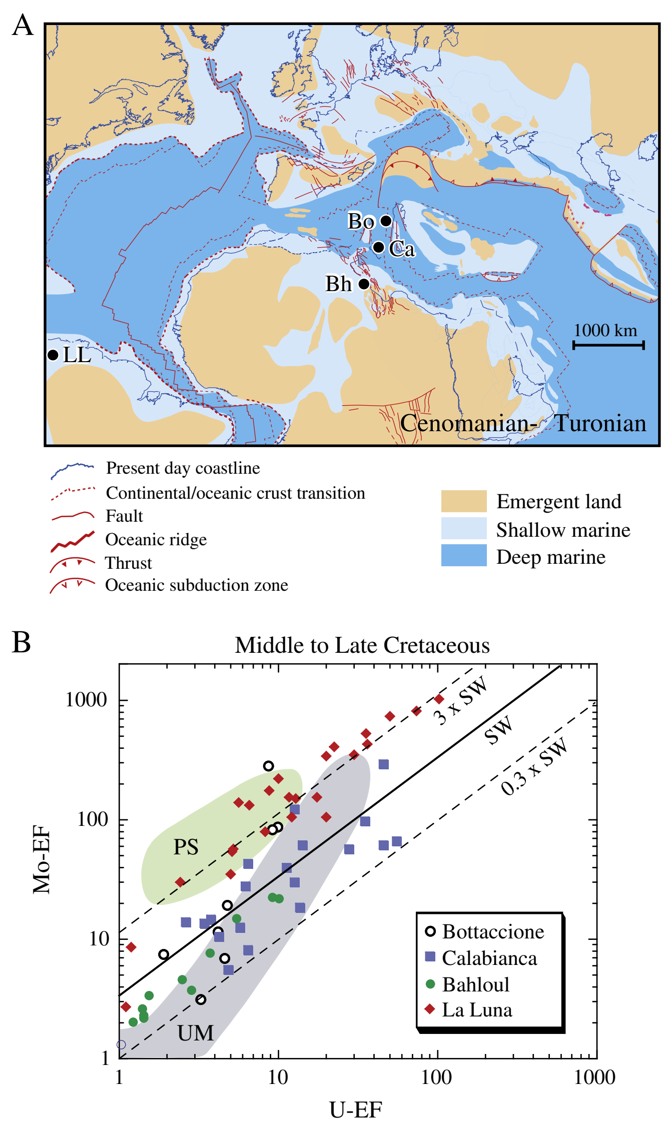

Fig. 6. (A) Paleogeographic reconstruction of the western Tethyan region during the Cenomanian (Middle Cretaceous). Redrawn from Barrier and Vrielynck (2008). (B) U–EF vs. Mo–EF for OAE-2 samples from (i) the Livello Bonarelli of the Bottaccione section (Umbria–Marche Basin, central Italy) and age-equivalent units of (ii) the Calabianca section (Sicily; data from Scopelliti et al. (2006)) and (iii) the Bahloul section (Tunisia; data from Caron et al. (1999)). The late Albian–early Campanian (Late Cretaceous) La Luna Formation is from the Maracaibo Basin of Venezuela (data from Mongenot et al. (1996)). Abbreviations as in Fig. 1.

age from the latest Albian to the earliest Campanian thus encompassing both the Cenomanian–Turonian OAE-2 and the Coniacian–Santonian OAE-3 (Fig. 2). Data used in this study are from a Maracaibo Basin drill core (Mongenot et al., 1996). The Maracaibo Basin was characterized by high-productivity surface waters and the presence of bathymetric barriers (i.e. shallow sills) around the basin margins, both factors contributing to the development of strongly anoxic (euxinic) bottom waters (Mongenot et al., 1996; Rey et al., 2004). In drill cores from the basin, the La Luna Formation appears as an alternation of black or dark grey limestones and shaly limestones, thinly laminated and rich in organic matter.

2.2. Elemental data

Samples of the Kimmeridgian Argiles de Wimereux and Hauterivian La Charce Section were analyzed by ICP-AES (major and minor elements) and ICP-MS (trace elements) at the spectrochemical laboratory of the Centre de Recherches en Pétrographie et Géochimie of Vandœuvre-les-Nancy (French Centre National de la Recherche Scientifique). The samples were prepared by the usual protocol consisting of fusion with $LiBO_2+$ by HNO_3 dissolution. Precision and accuracy were both better than 1% (mean 0.5%) for major and minor elements and 5% for Mo and U, as checked by international standards and analysis of replicate samples (Carignan et al., 2001). Results are given in Table 1. For the remaining study units, geochemical data were taken from our earlier studies and other published literature (as noted above).

Enrichment factors (EF) were calculated as:

$$X_{EF} = \left[(X/Al)_{sample}/(X/Al)_{PAAS}\right] \quad (1)$$

where X and Al represent the weight percent concentrations of elements X and Al, respectively. Samples were normalized using the post-Archean average shale (PAAS) compositions of Taylor and McLennan (1985). Al normalization is commonly used to minimize the effects of variable dilution by carbonate or biogenic silica, although certain caveats apply to this approach (for a discussion, see van der Weijden et al. (2002) and Tribovillard et al. (2006)). The virtue of using enrichment factors is that any value larger than 1.0 points to elements that are enriched relative to their average crustal abundance.

Table 1
Geochemical data for the previously unpublished material used in this paper, namely, the Hauterivian La Charce Section (SE France) and the Tithonian Argiles de Wimereux Formation of Boulonnais (N-France). *bd* stands for below detection. Detection thresholds are 0.1 ppm and 0.01 ppm for Mo and U, respectively.

La Charce section				Argiles de Wimereux			
Sample #	Al2O3	U	Mo	Sample #	Al2O3	U	Mo
	%	ppm	ppm		%	ppm	ppm
LCH 255/256 A	5.7	1.8	0.7	AdeW 142A	10.45	2.51	0.94
LCH 255/256 B	7.61	2.2	0.8	AdeW 145A	12.09	3.02	0.57
LCH 255/256 C	8.51	2.8	0.7	AdeW 148A	11.20	3.37	bd
LCH 255/256 D	5.95	2.4	0.7	AdeW 149A	13.16	2.56	bd
LCH 255/256 E	4.54	1.8	0.6	AdeW 140	6.94	1.33	bd
LCH 287/288 A	4.89	1.8	0.2	AdeW 141A	8.40	2.32	0.50
LCH 287/288 B	5.26	1.9	0.2	AdeW 132A	8.32	1.97	0.49
LCH 287/288 C	7.61	2.6	0.4	AdeW 134A	6.45	1.37	0.73
LCH 287/288 D	4.78	1.8	0.7	AdeW 136	6.78	1.55	bd
LCH 287/288 E	3.21	1.4	0.5	AdeW 137	12.17	2.25	0.65
LCH 319/320 A	4.69	1.6	0.2				
LCH 319/320 B	8.1	2.3	0.4				
LCH 319/320 C	7.38	2.5	0.3				
LCH 319/320 D	7.83	2.4	0.4				
LCH 319/320 E	6.13	2.1	0.3				
LCH 350/351 A	7.26	2.5	0.4				
LCH 350/351 B	8.68	2.7	0.3				
LCH 350/351 C	10.66	4.1	0.4				
LCH 350/351 D	9.31	3.3	0.3				
LCH 350/351 E	6.93	2.2	0.4				

In practical terms, EFs >3 represent a detectable enrichment of an element over average crustal concentrations, and EFs >10 represent a moderate to strong degree of enrichment (Algeo and Tribovillard, 2009).

3. Results

3.1. Early Jurassic

Samples of the Whitby Mudstone Formation define several stratigraphically distinct clusters on a U–Mo crossplot (Fig. 3B). Samples from below and above the Toarcian OAE interval yield U–EFs close to 1.0 (i.e., no U_{auth} enrichment) and Mo–EFs up to ~10 with an average of 2.16 (standard deviation 2.44). Most samples from the Toarcian OAE interval exhibit some degree of U_{auth} and Mo_{auth} enrichment relative to these “background” samples. Samples from the upper *semicelatum* subzone and basal *exaratum* subzone show weak enrichments (U–EFs ~1–2 and Mo–EFs ~2–3), and those from the main part of the *exaratum* subzone show modest enrichments (U–EFs ~2–5, Mo–EFs ~4–8). Both of these subsets fall along the unrestricted marine trend (Fig. 3B). Samples from the overlying *falciferum* ammonite subzone show U–EFs of ~1–2 and Mo–EFs of ~6–14, yielding Mo:U ratios close to those of the particulate shuttle field but reflecting a lower overall degree of authigenic U–Mo enrichment compared to samples of the modern Cariaco Basin (Fig. 1).

3.2. Late Jurassic

Samples of the Kimmeridge Clay Formation (KCF) exhibit a well--defined pattern of U–Mo covariation (Fig. 4B). Mo_{auth} is substantially more enriched than U_{auth}, typically by a factor of >10× where Mo–EF is >20; even at low EFs, Mo_{auth} tends to be more enriched than U_{auth}. As a result, samples from these units show a pattern of U–Mo covariation that does not fall along the unrestricted marine trend but, rather, rises toward and bisects the particulate shuttle field (Fig. 4B). Cycle 1 of the KCF yields lower U–EFs and Mo–EFs than Cycles 2 and 3, and Cycle 2 yields higher Mo–EFs (but similar U–EFs) to Cycle 3. Samples from the Bancs Jumeaux Fm. show Mo–EFs mostly in the range of 2 to 5, but a subset yields Mo–EFs of >5 (to a maximum of ~25) and fall along a trend parallel to that of KCF-Cycle 1 samples (although shifted toward lower U–EF values). Samples from the Argiles de Wimereux Fm. show only weak U–Mo enrichment (EFs <2). The Kashpir Oil Shales show substantial enrichments of both U_{auth} and Mo_{auth}, with EFs ranging from ~10 to 1000 (Fig. 4C). Samples having EFs <40 plot within the unrestricted marine field, and samples having EFs >40 trace an extension of this field although with authigenic Mo:U ratios that are somewhat higher (~2–3 × SW) than for lower-EF samples (mostly 0.3 to 1.0 × SW). The five samples containing highly sulfurized organic matter and corresponding to the most reducing depositional conditions (Riboulleau et al., 2003) have U–EFs of >20 and Mo–EFs >200.

3.3. Early Cretaceous

Most samples of the Fiume-Bosso Section show modest enrichments of authigenic U and Mo, with maximum EFs of ~20 for both elements (Fig. 5B). The samples do not exhibit a well-defined pattern of U–Mo covariation but, rather, broadly bracket the unrestricted marine trend. Samples of both the Veveyse de Châtel-Saint-Denis (VCD) and Angles sections exhibit low EFs for both U and Mo (<3), but a subset of samples exhibit higher Mo–EFs (to ~20) and fall along a vector in the direction of the particulate shuttle field (but without exhibiting the degree of U–Mo enrichment shown by the modern Cariaco Basin; Fig. 1). Samples of the La Charce Section exhibit uniformly low EFs for both U and Mo (<3), with slight enrichment of U_{auth} relative to Mo_{auth}.

3.4. Middle to Late Cretaceous

All four study units of Middle to Late Cretaceous age exhibit significant positive covariation between U–EF and Mo–EF, although Mo:U ratios and maximum EFs vary between the studied units (Fig. 6B). Samples of the Bahloul Formation exhibit maximum EFs of ~10 for U_{auth} and ~20 for Mo_{auth} and plot within the unrestricted marine trend. Samples of the Calabianca Section exhibit maximum EFs of ~50 for U_{auth} and ~300 for Mo_{auth} and define a covariation pattern that broadly straddles the unrestricted marine trend (although with greater variance than exhibited by sediments of the modern eastern tropical Pacific; Fig. 1). Samples of the Bottaccione Section exhibit maximum EFs of ~10 for U_{auth} and ~300 for Mo_{auth} and define a covariation pattern that falls between the unrestricted marine trend and the particulate shuttle field. Samples of the La Luna Formation exhibit greater U–Mo enrichment than the other units, with maximum EFs of ~100 for U_{auth} and ~1000 for Mo_{auth}. This unit also exhibits the highest Mo:U ratios, resulting in most samples plotting either within the particulate shuttle field or along an extension of the field to higher EFs tracking the 3×SW Mo:U ratio (Fig. 6B).

4. Interpretation of paleomarine systems

4.1. Redox conditions in unrestricted marine systems

For sediments deposited in modern unrestricted marine systems, the relationships between paleoredox conditions and authigenic U–Mo enrichment are as follows: (1) oxic environments show at most minor enrichments in both U and Mo; (2) suboxic environments correspond to modest authigenic enrichments (EFs <10), with U–EFs often greater than Mo–EFs; and (3) anoxic to euxinic facies record strong enrichments (EFs >10), with greater enrichment of Mo_{auth} relative to U_{auth} at higher EFs (yielding progressively higher sediment Mo:U ratios; Fig. 1; Algeo and Tribovillard, 2009). Relative to the aqueous Mo:U ratio of present-day seawater (SW), sediment Mo:U ratios tend to be low (~0.3×SW) in suboxic environments, intermediate (~1×SW) in weakly anoxic environments, and high (~3×SW) in strongly euxinic environments (Fig. 1). Thus, more reducing water mass conditions promote enrichment of the sediment in both U_{auth} and Mo_{auth}, but the rate of Mo uptake increases faster than that of U. At high Mo:U ratios, the trend for unrestricted marine systems converges with that of restricted systems with an active particulate shuttle, probably because particulate shuttles become increasingly important in strongly euxinic systems regardless of the degree of water mass restriction.

These patterns provide a basis for evaluation of bottom water redox conditions in unrestricted paleomarine systems. A number of the studied units exhibits authigenic U–Mo concentrations consistent with deposition under predominantly suboxic conditions, including the *semicelatum* subzone of the Whitby Mudstone Formation (Fig. 3B), the Argiles de Wimereux Formation (Fig. 4B), the La Charce Section (Fig. 5B), and portions of other studied units. Suboxic to predominantly anoxic conditions existed during deposition of the *exaratum* subzone of the Whitby Mudstone Formation (Fig. 3B), the non-sulfurized portions of the Kashpir Oil Shales (Fig. 4C), the Livello Faraoni in the Fiume-Bosso Section (Fig. 5B), and the Livello Bonarelli at its three studied sites (Fig. 6B). Predominantly euxinic conditions existed during deposition of the sulfurized portions of the Kashpir Oil Shales (Fig. 4C) and portions of the Livello Bonarelli and the La Luna Formation that show maximum authigenic U–Mo enrichments (Fig. 6B).

Paleomarine systems exhibit some variation in the fidelity with which they track the modern unrestricted marine trend. Thus, the non-sulfurized samples of the Kashpir Oil Shales plot almost entirely within this trend (Fig. 4C), whereas Livello Faraoni samples from the Fiume-Bosso Section (Fig. 5B) and Livello Bonarelli samples from the Calabianca Section exhibit greater scatter around the trend (Fig. 6B).

The paleoredox interpretations of the studied units given above are in excellent agreement with existing interpretations in the literature based on a range of sedimentological, paleontological, palynological, and geochemical proxies. We cannot report exhaustively here on every argument used in the literature to assess the paleodepositional conditions independently from our approach but all the supporting papers are quoted below. The Hauterivian La Charce samples are enriched in neither U nor Mo, which is in agreement with their depositional conditions, interpreted as being oxic to faintly suboxic by Baudin et al. (1999) and Van de Schootbrugge et al. (2000, 2003) who used geochemical (mainly P distribution) and isotopic arguments. Most of the (hemi-) pelagic sections containing the Faraoni Level typically illustrate the "shuttle effect" affecting Mo but not U, as was also the case for the Toarcian black shales presented above. It suggests that the three sections encompassing the Faraoni Level record suboxic depositional conditions with anoxia developing at some depth below the sediment–water interface as explained above. This is in good agreement with the interpretations of Baudin et al. (2002), Bodin et al. (2006, 2007, 2009) and Godet et al. (2006, 2008), who also concluded that the redox conditions documented by the three sections containing the Faraoni Level were not strongly reducing (using organic matter, clay-mineral, isotope and elemental data). However we observe here that a number of samples of the Fiume-Bosso Section recorded more severe redox conditions, which must be ascribed to the deep setting of this section.

The Kashpir Oil Shales are regarded as having been deposited in an unrestricted marine environment characterized by high surface water productivity and benthic redox conditions that regularly fluctuated between oxic and anoxic (Vishnevskaya et al., 1999; Riboulleau, 2000; Riboulleau et al., 1998, 2003, notably using organic geochemistry and palynofacies data). The patterns of authigenic U–Mo covariation documented here are consistent with this interpretation, although all samples show levels of enrichment that imply the existence of at least weakly anoxic conditions during their accumulation. It is possible that variation between oxic and anoxic conditions in the depositional environment occurred at timescales shorter than that represented by individual samples (~10^3 years), and that the trace metal content of the sediment reflects the anoxic episodes. In addition, the five samples combining high U–EF and the highest Mo–EF correspond to sediments where isorenieratene molecules have been detected. These molecular biomarkers evidence the presence of green sulfur bacteria performing anoxygenic photosynthesis in H_2S-containing water (within the photic zone). In other words, organic geochemistry data confirm our interpretation basing on U–Mo relationship that these five samples record euxinic conditions.

Among the three sections representing the early Late Cretaceous OAE-2, the deepwater environments (Bottaccione and Calabianca) show larger enrichment of U_{auth} and Mo_{auth} than the shallow platform setting of the Bahloul Formation. These results are consistent with previous works (Jenkyns, 1980; Arthur and Premoli-Silva, 1982; Coccioni et al., 1991; Scopelliti et al., 2004; Tsikos et al., 2004; Scopelliti et al., 2006; Turgeon and Brumsack, 2006; Mort et al., 2007) concluding that both deepwater sections endured strongly reducing conditions. The Calabianca and Bahloul sections show no evidence of operation of a particulate shuttle, whereas the slightly higher Mo:U ratios of the Bottaccione Section may reflect a weak or intermittently operating shuttle. On the other hand, the pattern of U–Mo covariation shown by the La Luna Formation is consistent with a strong particulate shuttle, operating over a wide range of redox conditions, probably ranging from suboxic to strongly euxinic (Mongenot et al., 1996; Alberdi and Tocco, 1999; Erlich et al., 1999a, 1999b, 2000; Lo Mónaco et al., 2002; Rey et al., 2004, the authors using paleontological, sedimentological, and geochemical—organic and inorganic—data).

One feature that, in combination with authigenic U–Mo enrichment, may assist in evaluating redox conditions in paleomarine systems is the presence of sulfurized organic matter. Several of the study units, including the La Luna Formation, KCF, and Kashpir Oil shales, contain at least some samples that yield high EFs (especially for Mo) in combination with highly sulfurized organic matter (Tribovillard et al., 2004). The same relationship pertains to sediments of the modern Peru Margin (Fig. 1), in which the significance of abundant sulfurized organic matter has been investigated (Mossmann et al., 1991; Eglinton et al., 1994; Lückge et al., 1996). This observation may be explained by the fact that sulfurized organic matter is known to enhance Mo uptake by the sediment (Tribovillard et al., 2004), and that open-marine conditions allow Mo to be continuously replenished to the oxygen-depleted bottom waters. Both high EFs and abundant sulfurized organic matter are a reflection of the high activity of HS^- in strongly euxinic environments. This relationship may also prove useful in predicting which samples are likely to contain S-rich organic matter prior to any labor-intensive and costly kerogen isolation and molecular analysis.

The U–EF vs. Mo–EF graph uses only concentrations in Al, U and Mo, and it leads to the same interpretations as those obtained with multi-parameter datasets. Notably, the approach developed here does not require information about organic matter; it may be used even if organic matter data are simply not available or even impossible to determine, as is the case with deeply buried rocks. In the case of organic matter overmaturation induced by deep burial or tectonics, organic matter data may not be measurable, whereas trace metal abundance can still be used (e.g., Mongenot et al., 1996; Ross and Bustin, 2009). Thus, when information about organic matter is not available for any reason, the U–EF vs. Mo–EF crossplot is a reliable alternative to the approach based on the relationship of total organic carbon to Mo concentration developed recently by Algeo and Lyons (2006) and Algeo et al. (2007). However, U may undergo some limited maturation control. Although not the most common trace metal present in hydrocarbons, U may be engaged into petroleum when source rocks reach the maturity stage corresponding to the so-called oil window (Bell, 1960). Consequently some U may be lost from the initial sedimentary rock when hydrocarbons are sourced and migrate. As suggested by P.B. Wignall (personal communication during review process), this may explain why some of the Whitby Mudstone (Early Jurassic) samples have so low U–EF values (<2).

4.2. Operation of water column particulate shuttles

A number of the study units exhibits patterns of authigenic U–Mo enrichment that are consistent with the operation of a vigorous metal-oxyhydroxide particulate shuttle within the water column. This process accelerates the transfer of aqueous Mo to the sediment while having little effect on aqueous U (see Section 1), thus resulting in markedly higher sediment Mo:U ratios over a wide range of EFs than are typical of unrestricted marine systems lacking an active particulate shuttle (Fig. 1). In the modern Cariaco Basin as well as in several of the paleomarine systems of the present study, Mo–EFs initially rise rapidly to >10 while U–EFs remain low (<3). For Mo–EFs higher than ~10, EFs for both Mo and U tend to increase in equal proportion (on a logarithmic scale), yielding sediment Mo:U ratios between 3 and 10 × SW (PS field, Fig. 1). At U–EFs >20 and Mo–EFs >200, samples deposited in such systems show EFs that converge with those of strongly anoxic unrestricted marine settings. This convergence may indicate that particulate shuttles enhancing aqueous Mo uptake by the sediment become increasing important in euxinic systems regardless of the degree of water mass restriction.

Among the present studied units, the Whitby Mudstone Formation shows evidence of an active particulate shuttle during deposition of shales of the *falciferum* subzone (Fig. 3B). The level of Mo_{auth} enrichment does not rise to that of the modern Cariaco Basin, possibly indicating a comparatively weak particulate shuttle in the Early Jurassic Cleveland Basin. A particulate shuttle may have existed also during deposition of Late Jurassic shales of the Bancs Jumeaux Formation (Fig. 4B) and Early Cretaceous shales of the Livello Faraoni in the Angles and VCD sections (Fig. 5B). The study units that exhibit the most characteristic patterns for a strong particulate shuttle are the Late Jurassic KCF (Fig. 4B) and the Late Cretaceous La Luna Formation (Fig. 6B). In both of these units, samples trace a vector of authigenic U–Mo enrichment that bisects the "particulate shuttle" field defined by the modern Cariaco Basin (Fig. 1). The particulate shuttle appears to have operated through multiple cycles of the KCF although with varying intensities, which is strongest during deposition of Cycle 2 and weakest during Cycle 1 (Fig. 4B). Particulate shuttle vigor appears to have been related to redox conditions, since Cycle 1 is inferred to represent the least reducing (i.e., suboxic) and Cycle 2 the most reducing (i.e., anoxic) conditions (Ramanampisoa et al., 1992; Tribovillard et al., 1994; Lallier-Vergès et al., 1997; Tribovillard et al., 2005). For the KCF our results may be compared to those of Pearce et al.'s (2010) who studied the formation in the Dorset (UK). Their results are presented using both a U–EF vs. Mo–EF diagram and a [TOC] vs. [Mo] crossplot (Pearce et al., 2010, their Fig. 4). The results for the Dorset and Cleveland datasets are consistent. For the Dorset, the Mo concentrations do not exceed the value of 70 ppm whereas they exceed 200 ppm for some samples of Cycle 2 of Cleveland (Fig. 7A). For values below [Mo] = 70 ppm, the two datasets show the same distribution in both the U–EF vs. Mo–EF and [TOC] vs. [Mo] diagrams. The difference between the two datasets is that Cycle 2 of Cleveland shows Mo concentrations exceeding 100 ppm (Fig. 7A). It may be reminded that these Mo-rich samples contain abundant organic sulfur as evoked above (Section 4.1). The consistency of the two datasets suggests that marine conditions were similar for both locations for the part of the "KCF Sea" that covered the domain corresponding to present-day England.

In the case of the La Luna Formation, the particulate shuttle appears to have operated vigorously for almost the full stratigraphic interval represented by our samples, with exceedingly strong euxinia leading to higher levels of authigenic U–Mo enrichment than observed in the modern Cariaco Basin (Fig. 6B; Mongenot et al., 1996; Alberdi and Tocco, 1999; Lo Mónaco et al., 2002). Thus, the degree of authigenic U–Mo enrichment in marine systems having an active particulate shuttle is influenced by redox conditions.

4.3. Evaluation of water mass restriction

The degree of deepwater restriction has the potential to influence authigenic U–Mo enrichment of marine sediments. Other variables being equal, increasing restriction results in lesser degrees of trace metal enrichment in sediments owing to a reduced resupply of aqueous trace metal species to the basinal water mass from the global ocean (Algeo and Lyons, 2006). However, water mass restriction is often correlated with other environmental variables such as redox conditions, and more reducing conditions in a restricted basin (especially within the suboxic–anoxic redox range) may enhance trace metal uptake and offset the effects of increasing restriction (Algeo and Lyons, 2006). Thus, assessments of the hydrographic, aqueous chemical, and redox conditions of a particular paleomarine system are best undertaken using a combination of proxies and analytical approaches.

One example of using authigenic U–Mo data to assess water mass restriction is the Early Jurassic Cleveland Basin (Yorkshire, United Kingdom; Fig. 3A). Whitby Mudstone Formation samples show almost no U enrichment and relatively limited Mo enrichment despite inferred strongly anoxic (euxinic) conditions during some depositional intervals (especially within the *falciferum* subzone; Fig. 3B). This pattern is likely to be indicative of strong drawdown of aqueous Mo in the Cleveland Basin water mass as a consequence of massive transfer to the sediment (McArthur et al., 2008), a process termed the "basin reservoir effect" (Algeo, 2004; Algeo and Lyons, 2006). Consequently the approach basing on the authigenic U–Mo enrichment does not supply the same information as that given by the [TOC] vs. [Mo] diagram (Fig. 7B). With such a diagram, coupled to geochemical and isotopic data, McArthur et al. (2008, their Fig. 11) and Pearce et al. (2008, their Fig. 3) observed two

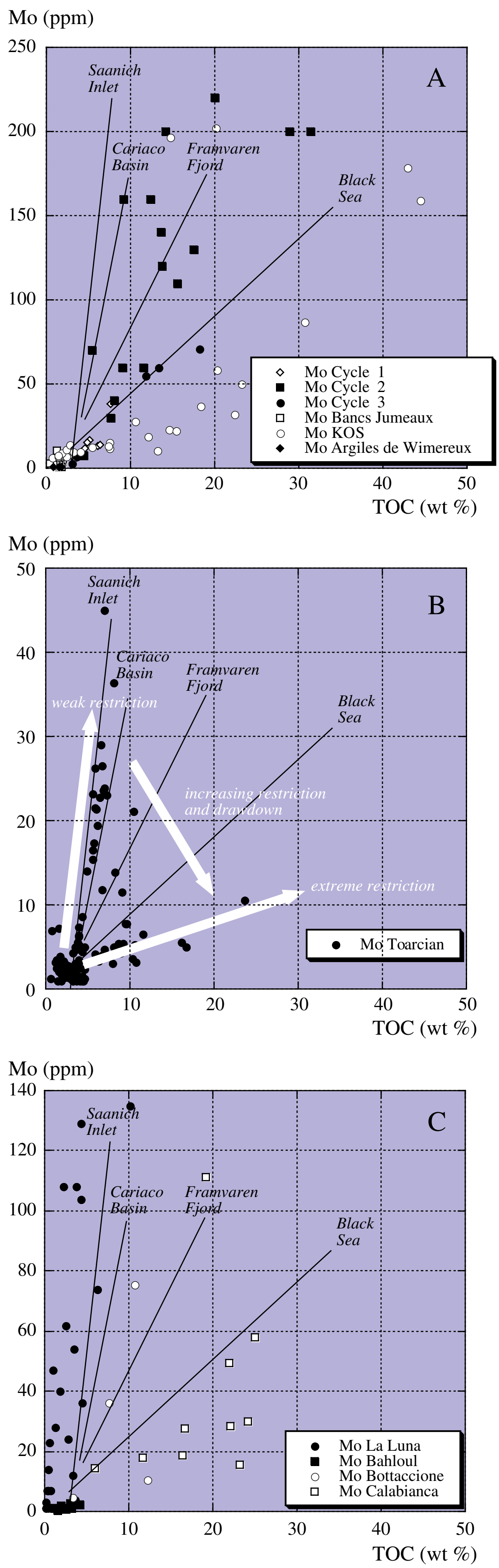

contrasting distributions for the Falciferum zone samples (Saanich Inlet-type distribution) and the Exaratum zone samples, showing a distribution beyond the Black Sea-type, that is, with very high TOCs and low Mo concentrations (Fig. 7B). Pearce et al. (2008) concluded to a regional anoxia affecting the Cleveland Basin during the Falciferum zone and widespread anoxia during the Exaratum zone, while McArthur et al. (2008) concluded weak water mass restriction during the Falciferum zone and extreme restriction during the Exaratum zone. With a U–EF vs. Mo–EF diagram, we cannot conclude to strong water mass restriction for the Exaratum zone because, in this specific case, the relatively low U–EF values place the samples close to the "unrestricted marine conditions" zone and not beyond it toward higher U–EF values as is the case for the Black Sea. Does this situation result from a "basin reservoir effect" also affecting the U inventory (which has not been reported yet), or from a loss of U during hydrocarbon generation as suggested above (end of Section 4.1), or does it relate to the length of time that the bottom waters were restricted for? We cannot conclude presently; we only observe that in the case of the Toarcian deposits of the Cleveland Basin, the U–EF vs. Mo–EF crossplot cannot assess unambiguously the water mass restriction conditions evidenced by previous studies. A different conclusion may be drawn from analysis of authigenic U–Mo data from the Late Cretaceous Maracaibo Basin of Venezuela (Fig. 6A). Previously, the Maracaibo Basin had been interpreted as strongly restricted because of its paleobathymetric configuration (Erlich et al., 2000). In a [TOC] vs. [Mo] diagram the La Luna samples show a "Saanich Inlet-type" distribution suggesting moderate water mass restriction (Fig. 7C). However, our data show that almost all La Luna Formation samples yield very high Mo–EFs (Fig. 6B), meaning that aqueous Mo was massively transferred to the sediment for a protracted (multi-million year) interval of time and, hence, must have been constantly replenished to the basinal water mass. If so, the deepwater mass of the basin could not have been isolated from the global ocean to any significant degree, probably because the marginal sills were not as continuous or as elevated as previously thought. Thus, comparisons of authigenic U–Mo data with other proxy data for paleomarine systems may help to clarify aspects of basin hydrography and water mass restriction.

4.4. Long-term changes in seawater trace metal concentrations

One additional factor that might influence authigenic U–Mo enrichment in marine sediments is changes in the concentration of aqueous U and Mo in seawater through time. Although the residence times of U and Mo in seawater are long (~450 and 780 kyr, respectively), some of the stratigraphic intervals of organic matter accumulation considered in this study lasted several million years (Fig. 2), suggesting that major changes in aqueous U and Mo concentrations could have occurred during these events. The idea of secular evolution of the trace metal inventories of seawater was first investigated by Algeo (2004) in relation to Late Devonian anoxic events, and probable drawdown of seawater trace metal concentrations has since been documented in conjunction with the Toarcian OAE (McArthur et al., 2008; Pearce et al., 2008) and the Cenomanian–Turonian OAE-2 (Hetzel et al., 2009). Whether these examples represent drawdown of trace metals in global seawater during Mesozoic OAEs, or merely changes in aqueous chemistry within restricted marine basins as for Devonian–Carboniferous black shales (Algeo et al., 2007; Rowe et al., 2008), remains unclear.

Fig. 7. Total organic carbon contents vs. Mo concentrations ([TOC] vs. [Mo]) diagrams drawn for most of the formations studied in this paper. A — Late Jurassic formations; B — Early Jurassic formations; C — Late Cretaceous formations. Note that the TOC data are not available for the two Italian Hauterivian sections. Such diagrams are designed to assess the paleodegree of water mass restriction in oxygen-limited marine basins (Algeo and Lyons, 2006; Algeo et al., 2007). The solid lines represent four present-day basins characterized by some restriction of the water mass circulation. The restriction severity increases from the Saanich Inlet to the Black Sea. See explanations in Algeo and Lyons (2006) and Algeo et al. (2007).

U–EF vs. Mo–EF crossplots (Figs. 3–6) are probably not optimal for assessing long-term variation in seawater trace metal concentrations, because simultaneous changes in U and Mo concentrations would result in positive covariant trends that mimic the effects of changing redox conditions on sediment trace metal enrichment (Fig. 1). A superior method of identifying secular changes in seawater trace metal concentrations utilizes Mo-TOC crossplots (Algeo and Lyons, 2006; Algeo et al., 2007), because an increase or decrease in the aqueous concentration of a given trace metal is likely to be manifested as an increase or decrease in the TOC-normalized concentration of that metal in the sediment. A second approach to this problem is based on chemostratigraphic trends for multiple trace metals in a single basin, variations in which are assessed relative to the secular redox and event history of the basin (Algeo and Maynard, 2008; Rowe et al., 2008; Hetzel et al., 2009). Although both approaches are subject to recording local water mass effects (e.g., the "basin reservoir effect" of Algeo and Lyons (2006)), it is at least conceptually possible to recognize a global signal. Such a signal might take the form of simultaneous changes of similar magnitudes in multiple, hydrographically independent basins—especially those in which deepwaters were subject to minimal restriction and, thus, have a trace metal composition close to that of normal seawater of a given age.

5. Conclusions

Patterns of authigenic U–Mo covariation in marine sediments provide insights regarding bottom water redox conditions, the operation of metal-oxyhydroxide particulate shuttles, and the degree of deepwater restriction. Organic-rich sediments of the western Tethyan region deposited during oceanic anoxic events (OAEs) of Early Jurassic to Late Cretaceous age exhibit characteristic U–Mo patterns. Our analysis generally confirms existing interpretations of redox conditions in these formations but provides significant new insights regarding water mass restriction and the operation of particulate shuttles in some depositional systems. In addition to allowing us to diagnose a spectrum between oxic and euxinic paleoconditions, the chart also helps determining the degree of water restriction for deposition in seaways, semi-restricted epicontinental seas or (semi-) enclosed basins. For instance, we conclude that the Maracaibo Basin, although configured as a semi-enclosed basin on the northern continental platform of South America during most of the Late Cretaceous never experienced restricted water mass circulation. These insights can help to address contentious issues pertaining to the character and origin of Mesozoic OAEs, such as the degree to which regional paleoceanographic factors controlled the development of the OAE.

Acknowledgments

We thank Giovanna Scopelliti and Stephane Bodin for kindly supplying data. Thanks to Tim Lyons for comments on an earlier version of the manuscript. Research by Thomas J. Algeo was supported by grants from the National Science Foundation (EAR-0618003 and EAR-0745574) and the University of Cincinnati Research Council. The useful reviews by Paul B. Wignall, Christopher R. Pearce and an anonymous reviewer, as well as the editorial work by the guest associate editor Jennifer L. Morford are much appreciated. Thanks to Neelima Dondapati, Journal Manager for Chemical Geology at Elsevier.

References

Alberdi, M., Tocco, R., 1999. Trace metals and organic geochemistry of the Machiques Member (Aptian–Albian) and La Luna Formation (Cenomanian–Campanian), Venezuela. Chemical Geology 160, 19–38.

Algeo, T.J., 2004. Can marine anoxic events draw down the trace-element inventory of seawater? Geology 32, 1057–1060.

Algeo, T.J., Lyons, T.W., 2006. Mo-total organic carbon covariation in modern anoxic marine environments: implication for analysis of paleoredox and paleohydrographic conditions. Paleoceanography 21, PA1016. doi:10.1029/2004PA001112.

Algeo, T.J., Maynard, J.B., 2004. Trace-element behavior and redox facies in core shales of Upper Pennsylvanian Kansas-type cyclothems. Chemical Geology 206, 289–318.

Algeo, T.J., Maynard, J.B., 2008. Trace metal covariation as a guide to water-mass conditions in ancient anoxic marine environments. Geosphere 4 (5), 872–887. doi:10.1130/GES00174.1.

Algeo, T.J., Tribovillard, N., 2009. Environmental analysis of paleoceanographic systems based on molybdenum–uranium covariation. Chemical Geology 268, 211–225.

Algeo, T.J., Lyons, T.W., Blakey, R.C., Over, D.J., 2007. Hydrographic conditions of the Devono–Carboniferous North American Seaway inferred from sedimentary Mo-TOC relationships. Palaeogeography, Palaeoclimatology, Palaeoecology 256, 204–230.

Arthur, M.A., Premoli Silva, I., 1982. Development of widespread organic carbon rich strata in the Mediterranean Tethys. In: Schlanger, S.O., Cita, M.B. (Eds.), Nature and Origin of Cretaceous Carbon-Rich Facies. Academic Press, London, pp. 7–54.

Barrier, E., Vrielynck, B., 2008. Palaeotectonic maps of the Middle East, CCGM, 14 maps.

Baudin, F., Bulot, L.G., Cecca, F., Coccioni, R., Gardin, S., Renard, M., 1999. Un équivalent du "Niveau Faraoni" dans le Bassin du Sud-Est de la France, indice possible d'un événement anoxique fini-hauterivien étendu à la Téthys méditerranéenne. Bulletin de la Société Géologique de France 170, 487–498.

Baudin, F., Cecca, F., Galeotti, S., Coccioni, R., 2002. Palaeoenvironmental controls of the distribution of organic matter within a C-org-rich marker bed (Faraoni level, uppermost Hauterivian, central Italy). Eclogae Geologicae Helvetiae 95, 1–13.

Bell, K.G., 1960. Uranium and other trace elements in petroleum and rock asphalts. Geological Survey Professional Paper, 356 B, pp. 44–65.

Bodin, S., Godet, A., Föllmi, K.B., Vermeulen, J., Arnaud, H., Strasser, A., Fiet, N., Adatte, T., 2006. The late Hauterivian Faraoni oceanic anoxic event in the western Tethys: evidence from phosphorus burial rates. Palaeogeography, Palaeoclimatology, Palaeoecology 235, 245–264.

Bodin, S., Godet, A., Matera, V., Steinmann, P., Vermeulen, J., Gardin, S., Adatte, T., Coccioni, R., Föllmi, K.B., 2007. Enrichment of redox-sensitive trace metals (U, V, Mo, As) associated with the late Hauterivian Faraoni oceanic anoxic event. International Journal of Earth Sciences 96, 327–341.

Bodin, S., Fiet, N., Godet, A., Matera, V., Westermann, S., Clément, A., Janssen, N.M.M., Stille, P., Föllmi, K.B., 2009. Early Cretaceous (late Berriasian to early Aptian) palaeoceanographic change along the northwestern Tethyan margin (Vocontian Trough, southeastern France): δ13C, δ18O and Sr-isotope belemnite and whole-rock records. Cretaceous Research 30, 1247–1262.

Bostick, B.C., Fendorf, S., Helz, G.R., 2003. Differential adsorption of molybdate and tetrathiomolybdate on pyrite (FeS_2). Environmental Sciences and Technologies 37, 285–291.

Brumsack, H.-J., 2006. The trace metal content of recent organic carbon-rich sediments: implications for Cretaceous black shale formation. Palaeogeography, Palaeoclimatology, Palaeoecology 232, 344–361.

Carignan, J., Hild, P., Morel, J., Yeghicheyan, D., 2001. Routine analysis of trace elements in geochemical samples using flow injection and low-pressure on-line liquid chromatography coupled to ICP-MS: a study of geochemical references materials BR, DR-N, UB-N, AN-G and GH. Geostandard Newsletter 25, 187–198.

Caron, M., Robaszynski, F., Amédro, F., Baudin, F., Deconinck, J.-F., Hochuli, P., Von Salis-Perch-Nielsen, K., Tribovillard, N., 1999. Estimation de la durée de l'événement anoxique global au passage Cénomanien/Turonien. Approche cyclostratigraphique dans la Formation Bahloul en Tunisie centrale. Bulletin de la Societe Geologique de France 170 (2), 145–160.

Cecca, F., Marini, A., Pallini, G., Baudin, F., Begouen, V., 1994. A guide-level of the uppermost Hauterivian (Lower Cretaceous) in the pelagic succession of Umbria–Marche Apennines (Central Italy): the Faraoni Level. Rivista Italiana Paleontologia e Stratigrafia 99, 551–568.

Chaillou, G., Anschutz, P., Lavaux, G., Schäfer, J., Blanc, G., 2002. The distribution of Mo, U, and Cd in relation to major redox species in muddy sediments of the Bay of Biscay. Marine Chemistry 80, 41–59.

Coccioni, R., Erba, E., Premoli Silva, I., 1991. Litho- and biostratigraphy of the Livello Bonarelli close to the Cenomanian/Turonian boundary (Umbria–Marche Apennines, Italy) and possible paleoceanographic significance. Colloque International sur les Évènements de la Limite Cénomanien/Turonien, Grenoble, 24–26 Mai 1991: Géologie Alpine, Mémoire H.S., 17, pp. 25–26.

Cohen, A.S., Coe, A.L., Harding, S.M., Schwark, L., 2004. Osmium isotope evidence for the regulation of atmospheric CO_2 by continental weathering. Geology 32, 157–160.

Crusius, J., Calvert, S., Pedersen, T., Sage, D., 1996. Rhenium and molybdenum enrichments in sediments as indicators of oxic, suboxic, and sulfidic conditions of deposition. Earth and Planetary Science Letters 145, 65–78.

Dean, W.E., Piper, D.Z., Peterson, L.C., 1999. Molybdenum accumulation in Cariaco basin sediment over the last 24 ky: a record of water-column anoxia and climate. Geology 27, 507–510.

Deconinck, J.-F., Geyssant, J.R., Proust, J.-N., Vidier, J.P., 1996. Sédimentologie et biostratigraphie des dépôts kimméridgiens et tithoniens du Boulonnais. Annales de la Société Géologique du Nord 4, 157–170.

Dellwig, O., Leipe, T., März, C., Glockzin, Pollehne, F., Schnetger, B., Yakushev, E.V., Böttcher, M.E., Brumsack, H.-J., 2010. A new particulate Mn–Fe–P-shuttle at the redoxcline of anoxic basins. Geochimica et Cosmochimica Acta 74, 7100–7115.

Eglinton, T.I., Irvine, J.E., Vairavamurthy, A., Zhou, W., Manowitz, B., 1994. Formation and diagenesis of macromolecular organic sulfur in Peru Margin sediments. Organic Geochemistry 22, 781–799.

Emerson, S.R., Huested, S.S., 1991. Ocean anoxia and the concentration of molybdenum and vanadium in seawater. Marine Chemistry 34, 177–196.

Erickson, B.E., Helz, G.R., 2000. Molybdenum (VI) speciation in sulfidic waters: stability and lability of thiomolybdates. Geochimica et Cosmochimica Acta 64, 1149–1158.
Erlich, R.N., Macsotay, O., Nederbragt, A.J., Lorente, M.A., 1999a. Palaeoecology, palaeogeography and depositional environments of Upper Cretaceous rocks of western Venezuela. Palaeogeography, Palaeoclimatology, Palaeoecology 153, 203–238.
Erlich, R.N., Palmer-Koleman, S.E., Antonieta Lorente, M., 1999b. Geochemical characterization of oceanographic and climatic changes recorded in upper Albian to lower Maastrichtian strata, western Venezuela. Cretaceous Research 20, 547–581.
Erlich, R.N., Macsotay, O., Nederbragt, A.J., Antonieta Lorente, M., 2000. Birth and death of the Late Cretaceous "La Luna Sea", and origin of the Tres Esquinas phosphorites. Journal of South American Earth Sciences 13, 21–45.
Godet, A., Bodin, S., Föllmi, K.B., Vermeulen, J., Gardin, S., Fiet, N., Adatte, T., Zsolt, B., Stüben, D., van de Schootbrugge, B., 2006. Evolution of the marine stable carbon-isotope record during the early Cretaceous: a focus on the late Hauterivian and Barremian in the Tethyan realm. Earth and Planetary Science Letters 242, 254–271.
Godet, A., Bodin, S., Adatte, T., Föllmi, K.B., 2008. Platform-induced clay-mineral fractionation along a northern Tethyan basin-platform transect: implications for the interpretation of Early Cretaceous climate change (Late Hauterivian–Early Aptian). Cretaceous Research 23, 830–847.
Helz, G.R., Miller, C.V., Charnock, J.M., Mosselmans, J.L.W., Pattrick, R.A.D., Garner, C.D., Vaughan, D.J., 1996. Mechanisms of molybdenum removal from the sea and its concentration in black shales: EXAFS evidences. Geochimica et Cosmochimica Acta 60, 3631–3642.
Helz, G.R., Bura-Nakić, E., Mikac, N., Ciglenečki, I., 2011. New model for molybdenum behavior in euxinic waters. Chemical Geology 284, 323–332.
Hetzel, A., Böttcher, M.E., Wortmann, U.G., Brumsack, H.-J., 2009. Paleo-redox conditions during OAE 2 reflected in Demerara Rise sediment geochemistry (ODP Leg 207). Palaeogeography, Palaeoclimatology, Palaeoecology 273, 302–328.
Jenkyns, H.C., 1980. Cretaceous anoxic events from continents to oceans. Journal of the Geological Society of London 137, 171–188.
Jenkyns, H.C., 2010. Geochemistry of oceanic anoxic events. Geochemistry, Geophysics, Geosystems 11, Q03004. doi:10.1029/2009GC002788.
Jenkyns, H.C., Jones, C.E., Gröcke, D.R., Hesselbo, S.P., Parkinson, D.N., 2002. Chemostratigraphy of the Jurassic system: applications, limitations and implication for palaeoceanography. Journal of the Geological Society 159, 351–378.
Klinkhammer, G.P., Palmer, M.R., 1991. Uranium in the oceans: where it goes and why. Geochimica et Cosmochimica Acta 55, 1799–1806.
Lallier-Vergès, E., Hayes, J., Tribovillard, N., Zaback, D., Connan, J., Bertrand, P., 1997. Productivity-induced cyclic sulfur enrichment of hydrocarbon-rich sediments from the Kimmeridge Clay Formation. Chemical Geology 134, 277–288.
Lo Mónaco, S., López, L., Rojas, H., Garcia, D., Premovic, P., Briceño, H., 2002. Distribution of major and trace elements in La Luna Formation, Southwestern Venezuelan Basin. Organic Geochemistry 33, 1593–1608.
Lückge, A., Boussafir, M., Lallier-Vergès, E., Littke, R., 1996. Comparative study of organic matter preservation in immature sediments along the continental margins of Peru and Oman. Part I: results of petrographical and bulk geochemical data. Organic Geochemistry 24, 437–451.
Lyons, T.W., Werne, J.P., Hollander, D.J., Murray, R.W., 2003. Contrasting sulfur geochemistry and Fe/Al and Mo/Al ratios across the last oxic-to-anoxic transition in the Cariaco Basin, Venezuela. Chemical Geology 195, 131–157.
Lyons, T.W., Anbar, A.D., Severmann, S., Scott, C., Gill, B.C., 2009. Tracking euxinia in the ancient ocean: a multiproxy perspective and Proterozoic case study. Annual Review of Earth and Planetary Sciences 37, 507–534.
Marcellari, C.E., De Vries, T.J., 1987. Late Cretaceous upwelling and anoxic sedimentation in Northwestern South America. Palaeogeography, Palaeoclimatology, Palaeoecology 59, 279–292.
McArthur, J.M., Algeo, T.J., van de Schootbrugge, B., Li, Q., Howarth, R.J., 2008. Basinal restriction, black shales, Re–Os dating, and the Early Toarcian (Jurassic) oceanic anoxic event. Paleoceanography 23, PA4217. doi:10.1029/2008PA001607.
McLennan, S.M., 2001. Relationships between the trace element composition of sedimentary rocks and upper continental crust. Geochemistry, Geophysics, Geosystems 2 2000GC000109.
McManus, J., Berelson, W.M., Klinkhammer, G.P., Hammond, D.E., Holm, C., 2005. Authigenic uranium: relationship to oxygen penetration depth and organic carbon rain. Geochimica et Cosmochimica Acta 69, 95–108.
McManus, J., Berelson, W.B., Severmann, S., Poulson, R.L., Hammond, D.E., Klinkhammer, G.P., Holm, C., 2006. Molybdenum and uranium geochemistry in continental margin sediments: paleoproxy potential. Geochimica et Cosmochimica Acta 70, 4643–4662.
Mongenot, T., Tribovillard, N., Desprairies, A., Lallier-Vergès, E., Laggoun-Defarge, F., 1996. Trace elements as paleoenvironmental markers in strongly mature hydrocarbon source rocks: the Cretaceous La Luna Formation of Venezuela. Sedimentary Geology 103, 23–37.
Morford, J.L., Emerson, S., 1999. The geochemistry of redox sensitive trace metals in sediments. Geochimica et Cosmochimica Acta 63, 1735–1750.
Morford, J.L., Emerson, S.R., Breckel, E.J., Kim, S.H., 2005. Diagenesis of oxyanions (V, U, Re, and Mo) in pore waters and sediments from a continental margin. Geochimica et Cosmochimica Acta 69, 5021–5032.
Morford, J.L., Martin, W.R., Francois, R., Carney, C.M., 2009. A model for uranium, rhenium, and molybdenum diagenesis in marine sediments based on results from coastal locations. Geochimica et Cosmochimica Acta 73, 2938–2960.
Mort, H., Jacquat, O., Adatte, T., Steinmann, P., Föllmi, K., Matera, V., Berner, Z., Stüben, D., 2007. The Cenomanian/Turonian anoxic event at the Bonarelli Level in Italy and Spain: enhanced productivity and/or better preservation? Cretaceous Research 28, 597–612.
Mossmann, J.-R., Aplin, A.C., Curtis, C.D., Coleman, M.L., 1991. Geochemistry of inorganic and organic sulphur in organic-rich sediments from the Peru margin. Geochimica et Cosmochimica Acta 55, 3581–3595.
Pearce, C.R., Cohen, A.S., Coe, A.L., Burton, K.W., 2008. Molybdenum isotope evidence for global ocean anoxia coupled with perturbations to the carbon cycle during the Early Jurassic. Geology 36, 231–234.
Pearce, C.R., Coe, A.L., Cohen, A.S., 2010. Seawater redox variations during the deposition of the Kimmeridge Clay Formation, United Kingdom (Upper Jurassic): evidence from molybdenum isotopes and trace metal ratios. Paleoceanography 25, PA4213. doi:10.1029/2010PA001963.
Piper, D.Z., Calvert, S.E., 2009. A marine biogeochemical perspective on black shale deposition. Earth-Science Reviews 95, 63–96.
Poulson Brucker, R.L., McManus, J., Severmann, S., Berelson, W.M., 2009. Molybdenum behavior during early diagenesis: Insights from Mo isotopes. Geochemistry, Geophysics, Geosystems 10 (6). doi:10.1029/2008GC002180.
Proust, J.-N., Deconinck, J.-F., Geyssant, J.R., Herbin, J.-P., Vidier, J.P., 1995. Sequence analytical approach to the Upper Kimmeridgian–Lower Tithonian storm-dominated ramp deposits of the Boulonnais (Northern France). A landward time-equivalent to offshore marine source rocks. Geologische Rundschau 84, 255–271.
Ramanampisoa, L., Bertrand, P., Disnar, J.R., Lallier-Vergès, E., Pradier, B., Tribovillard, N., 1992. Etude à haute résolution d'un cycle du carbone organique de roches kimméridgiennes du Yorkshire (Grande-Bretagne): résultats préliminaires de géochimie et de pétrographie organique. Comptes Rendus de l'Académie des Sciences 314, 1493–1498.
Rey, O., Simo, J.A., Lorente, M.A., 2004. A record of long- and short-term environmental and climatic change during OAE3: La Luna Formation, Late Cretaceous (Santonian–Early Campanian), Venezuela. Sedimentary Geology 170, 85–105.
Riboulleau, A., 2000. Géochimie des black shales du Jurassique supérieur de la plate-forme russe. Processus de sédimentation et de préservation de la matière organique. PhD Thesis, Université Pierre et Marie Curie, Paris VI, 262 pp.
Riboulleau, A., Baudin, F., Daux, V., Hantzpergue, P., Renard, M., Zakharov, V., 1998. Evolution de la paléotempérature des eaux de la plate-forme russe au cours du Jurassique Supérieur. Comptes Rendus de l'Académie des Sciences 326, 239–246.
Riboulleau, A., Baudin, F., Deconinck, J.-F., Derenne, S., Largeau, C., Tribovillard, N., 2003. Depositional conditions and organic matter preservation pathways in an epicontinental environment: the Upper Jurassic Kashpir Oil Shales (Volga Basin, Russia). Palaeogeography, Palaeoclimatology, Palaeoecology 197, 171–197.
Ross, D.J.K., Bustin, R.M., 2009. Investigating the use of sedimentary geochemical proxies for paleoenvironment interpretation of thermally mature organic-rich strata: examples from the Devonian–Mississippian shales, Western Canadian Sedimentary Basin. Chemical Geology 260, 1–19.
Rowe, H.D., Loucks, R.G., Ruppel, S.C., Rimmer, S.M., 2008. Mississippian Barnett Formation, Fort Worth Basin, Texas: bulk geochemical inferences and Mo-TOC constraints on the severity of hydrographic restriction. Chemical Geology 257, 16–25.
Scopelliti, G., Bellanca, A., Coccioni, R., Luciani, V., Neri, R., Baudin, F., Chiari, M., Marcucci, M., 2004. High-resolution geochemical and biotic records of the Tethyan Bonarelli Level (OAE2, Latest Cenomanian) from the Calabianca–Guidaloca composite section, northwestern Sicily, Italy. Palaeogeography, Palaeoclimatology, Palaeoecology 208, 293–317.
Scopelliti, G., Bellanca, A., Neri, R., Baudin, F., Coccioni, R., 2006. Comparative high-resolution chemostratigraphy of the Bonarelli Level from the reference Bottaccione section (Umbria–Marche Apennines) and from an equivalent section in NW Sicily: consistent and contrasting responses to the OAE2. Chemical Geology 228, 266–285.
Soua, M., Tribovillard, N., 2007. Modèle de dépôt pour le passage Cénomanien-Turonien: exemple de la formation Bahloul en Tunisie. Comptes Rendus Géosciences 339, 692–701.
Suan, G., Pittet, B., Bour, Y., Mattioli, E., Duarte, L.V., Mailliot, S., 2008. Duration of the Early Toarcian carbon isotope excursion deduced from spectral analysis: consequence for its possible causes. Earth and Planetary Science Letters 267, 666–679.
Suan, G., Mattioli, E., Pittet, B., Lécuyer, C., Suchéras-Marx, B., Duarte, L.V., Philippe, M., Reggiani, L., Martineau, F., 2010. Secular environmental precursors to Early Toarcian (Jurassic) extreme climate changes. Earth and Planetary Science Letters 290, 448–458.
Taylor, S.R., McLennan, S.M., 1985. The Continental Crust: Its Composition and Evolution. Blackwell, Oxford. (312 pp.).
Tossell, J.A., 2005. Calculating the partitioning of the isotopes of Mo between oxidic and sulfidic species in aqueous solution. Geochimica Cosmochimica Acta 69, 2981–2993.
Tribovillard, N., Jautée, E., Stéphan, J.-F., Cotillon, P., Reyre, Y., Manivit, H., 1991. Cretaceous Black Shales of Venezuelan Andes. Preliminary results on stratigraphy and paleoenvironmental interpretations. Palaeogeography, Palaeoclimatology, Palaeoecology 81, 313–321.
Tribovillard, N., Desprairies, A., Lallier-Vergès, E., Moureau, N., Ramdani, A., Ramanampisoa, L., 1994. Geochemical study of organic-rich cycles from the Kimmeridge Clay Formation of Yorkshire (G.B.): productivity vs. anoxia. Palaeogeography, Palaeoclimatology, Palaeoecology 108, 165–181.
Tribovillard, N., Bialkowski, A., Tyson, R.V., Vergès, E., Deconinck, J.-F., 2001. Organic facies and sea level variation in the Late Kimmeridgian of the Boulonnais area (northernmost France). Marine and Petroleum Geology 18, 371–389.
Tribovillard, N., Averbuch, O., Bialkowski, A., Deconinck, J.-F., 2002. The influence of the early diagenesis of marine organic matter on the magnetic-susceptibility signal of sedimentary rock. Bulletin de la Societe Geologique de France 173, 295–306.
Tribovillard, N., Riboulleau, A., Lyons, T., Baudin, F., 2004. Enhanced trapping of molybdenum by sulfurized organic matter of marine origin as recorded by various Mesozoic formations. Chemical Geology 213, 385–401.
Tribovillard, N., Ramdani, A., Trentesaux, A., 2005. Controls on organic accumulation in Late Jurassic shales of Northwestern Europe as inferred from trace-metal geochemistry. In: Harris, N. (Ed.), The Deposition of Organic-Carbon-Rich Sediments: Models, Mechanisms, and Consequences: SEPM Special Publication, No. 82, pp. 145–164.

Tribovillard, N., Algeo, T., Lyons, T.W., Riboulleau, A., 2006. Trace metals as paleoredox and paleoproductivity proxies: an update. Chemical Geology 232, 12–32.
Tribovillard, N., Bout-Roumazeilles, V., Algeo, T.J., Lyons, T.W., Sionneau, T., Montero-Serrano, J.C., Riboulleau, A., Baudin, F., 2008a. Paleodepositional conditions in the Orca Basin as inferred from organic matter and trace metal contents. Marine Geology 254 (1/2), 62–72.
Tribovillard, N., Lyons, T.W., Riboulleau, A., Bout-Roumazeilles, V., 2008b. A possible capture of molybdenum during early diagenesis of dysoxic sediments. Bulletin de la Societe Geologique de France 179 (1), 3–12.
Tsikos, H., Jenkyns, H.C., Walsworth-Bell, B., Petrizzo, M.R., Forster, A., Kolonic, S., Erba, E., Premoli Silva, I., Baas, M., Wagner, T., Sinninghe Damsté, J.S., 2004. Carbon-isotope stratigraphy recorded by the Cenomanian/Turonian oceanic anoxic event: correlation and implications based on three key-localities. Journal of the Geological Society of London 161, 711–719.
Turgeon, S., Brumsack, H.-J., 2006. Anoxic vs. dysoxic events reflected in sediment geochemistry during the Cenomanian–Turonian Boundary Event (Cretaceous) in the Umbria–Marche Basin of Italy. Chemical Geology 234, 321–339.
Tyson, R.V., 2005. The “productivity versus preservation” controversy: cause, flaws, and resolution. In: Harris, N. (Ed.), The Deposition of Organic-Carbon-Rich Sediments: Models, Mechanisms, and Consequences: SEPM Special Publication, No. 82, pp. 17–33.
Van de Schootbrugge, B., Föllmi, K.B., Bulot, L.G., Burns, S.J., 2000. Paleoceanographic changes during the early Cretaceous (Valanginian–Hauterivian): evidence from oxygen and carbon stable isotopes. Earth and Planetary Science Letters 181, 15–31.
Van de Schootbrugge, B., Kuhn, O., Adatte, T., Steinmann, P., Föllmi, K., 2003. Decoupling of P- and C_{org}-burial following Early Cretaceous (Valanginian–Hauterivian) platform drowning along the NW Tethyan margin. Palaeogeography, Palaeoclimatology, Palaeoecology 199, 315–331.
van der Weijden, C.H., Reichart, G.J., van Os, B.J.H., 2002. Sedimentary trace element records over the last 200 kyr from within and below the northern Arabian Sea oxygen minimum zone. Marine Geology 231, 69–88.
Vishnevskaya, V.S., de Wever, P., Baraboshkin, E.Y., Bogdanov, N.A., Bragin, N.Y., Bragina, L.G., Kostyuchenko, A.S., Lambert, E., Malinovsky, Y.M., Sedaeva, K.M., Zukova, G.A., 1999. New stratigraphic and palaeogeographic data on Upper Jurassic to Cretaceous deposits from the eastern periphery of the Russian Platform (Russia). Geodiversitas 21, 347–363.
Vorlicek, T.P., Kahn, M.D., Kasuza, Y., Helz, G.R., 2004. Capture of molybdenum in pyrite-forming sediments: role of ligand-induced reduction by polysulfides. Geochimica et Cosmochimica Acta 68, 547–556.
Wignall, P.B., 1994. Black shales. Oxford Monographs on Geology and Geophysics, 30. Oxford Science Publication (127 pp.).
Wignall, P.B., Newton, R., 2001. Black shales on the basin margin: a model based on examples from the Upper Jurassic of the Boulonnais, northern France. Sedimentary Geology 144, 335–356.
Wignall, P.B., Newton, R.A., Little, C.T.S., 2005. The timing of paleoenvironmental change and cause-and-effect relationships during the Early Jurassic mass extinction in Europe. American Journal of Sciences 305, 1014–1032.
Zheng, Y., Anderson, R.F., van Geen, A., Kuwabara, J., 2000. Authigenic molybdenum formation in marine sediments: a link to pore water sulfide in the Santa Barbara Basin. Geochimica et Cosmochimica Acta 64, 4165–4178.
Zheng, Y., Anderson, R.F., van Geen, A., Fleisher, M.Q., 2002a. Preservation of non-lithogenic particulate uranium in marine sediments. Geochimica et Cosmochimica Acta 66, 3085–3092.
Zheng, Y., Anderson, R.F., van Geen, A., Fleisher, M.Q., 2002b. Remobilization of authigenic uranium in marine sediments by bioturbation. Geochimica et Cosmochimica Acta 66, 1759–1772.